J Mater Sci: Mater Med (2008) 19:2575–2580
DOI 10.1007/s10856-007-3202-7

The one-pot synthesis of dextran-based nanoparticles and their application in in-situ fabrication of dextran-magnetite nanocomposites

Hongjing Dou · Bin Xu · Ke Tao · Minhua Tang · Kang Sun

Received: 25 December 2006 / Accepted: 5 June 2007 / Published online: 1 August 2007

Abstract The dextran-based nanoparticles containing carboxyl groups were synthesized by a one-pot approach, without using any organic solvents and surfactants. The resultant dextran-based nanoparticles was used as a host for the growing and organization of Fe_3O_4 nanoparticles. The approach consists of the mixture of ferrous/ferric ions aqueous solution and host nanoparticles and subsequent coprecipitation of ferrous/ferric ions in basic medium. The magnetic nanocomposite material obtained was characterized using transmission electron microscopy (TEM), dynamic light scattering (DLS), thermogravimetric analysis (TGA), X-ray diffraction techniques (XRD) and vibrating sample magnetometry (VSM). The data demonstrate that the carboxyls which can capture cationic ferrous/ferric by electronic interaction in the dextran-based hosts plays a crucial role in fabricating nanocomposites with a homogeneous spatial distribution of magnetite nanoparticles. The magnetic nanocomposites exhibit comparable saturation magnetizations to that of reported Fe_3O_4 nanoparticles, and therefore display great potential in a large scope of biomedical fields.

Introduction

Polymeric nanoparticles stabilized with covalent linkage, especially those with functional groups simultaneously, have attracted extensive attention in recent years not only owing to their potential applications in large scope of fields but also for the fundamental scientific interests [1–4]. Water-soluble polysaccharide, due to their excellent biocompatibility and unique physicochemical properties, should be appropriate to preparing nanoparticles applicable in many fields, especially for biomedical purpose [5, 6]. Some recent studies focused on the fabrication of polysaccharide nanoparticles and great development has been achieved [1, 2, 7]. In previous works [8–10], we synthesized dextran-based and hydroxypropyl-based nanoparticles with interior carboxy groups by a facile one-step synthesis without using any organic solvents and surfactants.

The study on magnetite nanoparticles (MNPs) have been intensively pursued in recent years for their widely potential applications in biomedical fields [11–14], such as magnetic resonance image (MRI), hyperthermia, drug delivery, cell and DNA labeling, etc. However, the MNPs prepared either by coprecipitation method [15, 16] or by organometallic decomposition method [17–19] must be further modified for biomedical uses to provide them better biocompatibility and longer circulation in vivo [20]. It is difficult to synthesize the nanocomposites with magnetite nanoparticles embedded in polymeric host for the immiscibility between organic polymer and inorganic magnetite nanoparticles. In-situ synthesis provided a good solution to synthesize silica-based magnetic nanocomposites [21, 22] for its facility and effectivity. In this paper, we firstly apply this approach in realizing the integration of magnetite nanoparticles and dextran-based organic template.

Coprecipitation of ferrous/ferric ions in basic aqueous solutions is a facile approach to synthesize magnetite nanoparticles [23]. Herein, dextran-based nanoparticles containing carboxy groups (DANP) were firstly synthesized by using the one-pot approach we reported previously [8, 9]. Furthermore, dextran-based magnetic nanocomposites

H. Dou · B. Xu · K. Tao · M. Tang · K. Sun (✉)
State Key Lab of Metal Matrix Composites, Shanghai Jiao Tong University, Shanghai 200030, P.R. China
e-mail: ksun@sjtu.edu.cn

(denoted as DAMNP) were synthesized by coprecipitation approach using the DANP as a template, so that the magnetite nanoparticles can in-situ form inside the template as a result of the electronic interaction of carboxyls with the precursor ions of magnetites. The size, morphology, composition and magnetism of DAMNP were studied by various measurements.

Experimental section

Materials

Dextran (Shanghai Sinopharm Chemical Reagent Co.Ltd, weight-average molecular weight, $M_w = 1.15 \times 10^4$ g/mol) was used directly. Acrylic acid was vacuum distilled before use. *N*, *N*′-methylene bisacrylamide (MBA) (Fluka) was re-crystallized from methanol. Cerium (IV) ammonium nitrate (CAN) (Shanghai Sinopharm Chemical Reagent Co.Ltd) was recrystallized from dilute nitric acid containing appropriate ammonium nitrate. Analytical grade ferric chloride hexahydrate ($FeCl_3 \cdot 6H_2O$), ferrous chloride tetrahydrate ($FeCl_2 \cdot 4H_2O$), ammonia solution (25% wt) and dextran ($M_w \approx 20{,}000$) were purchased from Shanghai Sinopharm Chemical Reagent Co.Ltd and were used directly.

Synthesis of DANP

The DANP were synthesized by the process as follows: 2.5 mg dextran was dissolved in 50 mL deionized water at 25 under gentle stirring and nitrogen bubbling, then the solution of a designated amount of CAN in 1.25 mL 0.1 N nitric acid and a designated amount of AA were successively added. Twenty minutes later, MBA was added and the reaction was kept at 30 °C for 4 h. Thereafter, 1 M NaOH was added to neutralize the reaction system. Finally, the reaction solution was dialyzed against deionized water for 3 days using the membrane bag with a 14,000 cut-off molecular weight to remove the un-reacted monomers and the un-grafted PAA.

Synthesis of DAMNP

About 0.5 g DANP was dissolved in 75 mL deionized water and mixed with 50 mL of aqueous solution of 0.10 g $FeCl_2{\cdot}4H_2O$ and 0.27 g $FeCl_3{\cdot}6H_2O$ (mol^{2+}_{Fe}:mol^{3+}_{Fe} = 1:2). The mixture was kept under vigorously stirring (~1,000 rpm) and nitrogen bubbling for 15 min to permit the adsorption of ferrous/ferric ions into DANP. Then the mixture was added dropwise into 75 mL of 5% ammonia (weight percent) under stirring (~1,000 rpm) and nitrogen atmosphere. The pH value of the medium hence jumped to above 10 and simultaneously accompanied by a change of color from yellow to dark brown, indicating the formation of magnetite nanoparticles. The reaction continued for 1 h and then the reaction solution was dialyzed against distilled water for 3 days. The resultant DAMNP were collected by magnetic separation and succedent lyophilization. The whole process of the preparation of DANP and DAMNP is illustrated in Scheme 1.

Dynamic light scattering

Malvern Autosizer 4,700 Laser Light Scattering (LLS) spectrometer was used. DLS measurements were performed at a fixed scattering angle (θ) of 90°.

Morphology study

Transmission Electron Microscopy (TEM) (PHILIPS CM 120 BioTwin) was used to observe the morphology of nanoparticles. For TEM observations of DANP, the aqueous solutions of nanoparticles were placed onto carbon-coated copper grid and negative stained using phosphotungstic acid (5% (w/w)), and then dried at room temperature for 72 h. The DAMNP were observed directly after drying at room temperature for 72 h.

^1H NMR

^{1}H NMR measurements were carried out by MERCURY PLUS-400, VARIAN Co. The nanoparticles were solved in D_2O before measurement, and the pH value was adjusted by adding appropriate NaOD into the solution.

X-ray diffraction

The crystallite phase of the nanoparticles was identified by recording X-ray diffraction patterns (XRD) using a D8 Advance Diffractometer (Bruker, Germany) equipped with a Cu Kα radiation source.

Thermogravimetric analysis

The amount of macromolecule in DAMNP was determined by a thermogravimetric analyzer (TGA) using a TGA2050 (TA Instruments, USA) with a 20 °C/min heating rate under nitrogen atmosphere.

Magnetization measurements

The magnetization study was performed using a vibrating sample magnetometer (VSM) at room temperature.

Results and discussion

The hydrodynamic diameter distribution ($<D_h>$) and TEM image of DANP1 (synthesized at M_{GU}:M_{AA}:M_{Ce}:M_{MBA} =

Scheme 1 The schematic illustration of the synthesis of DANP and DAMNP

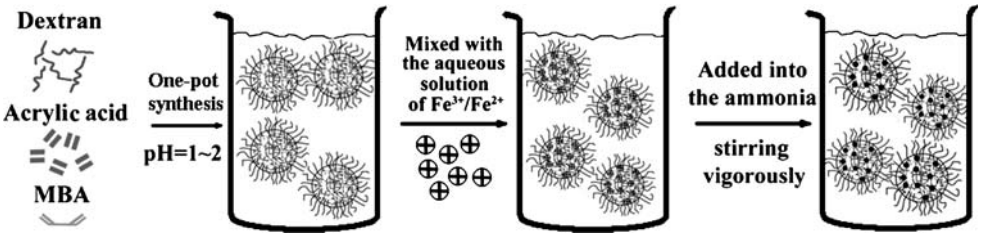

1:1:0.14:0.1, GU means glucose units) were shown in Fig. 1. DLS measurement reveals that DANP1 nanoparticles have an average hydrodynamic diameter of 200–300 nm. It is clear that the nanoparticles possess near spherical morphology with a dimension of ca.100 nm. The diameter of nanoparticles observed by TEM is slightly smaller than what determined by DLS, this decrease of size should be caused by the shrinkage of nanoparticles during water evaporation in the sample preparation, similar phenomenon was also observed in the morphology observation of other nanoparticles [24]. Figure 2 shows the ^{1}H NMR spectrum of DANP1, dextran and PAA. The signals around 4.8 ppm should be attributed to the 1H of dextran [25] and the signal from 1.0 to 2.2 ppm in spectrum of DANP1 can be mainly ascribed to the PAA segments in DANP1, which indicates the successful graft of PAA on the dextran chains

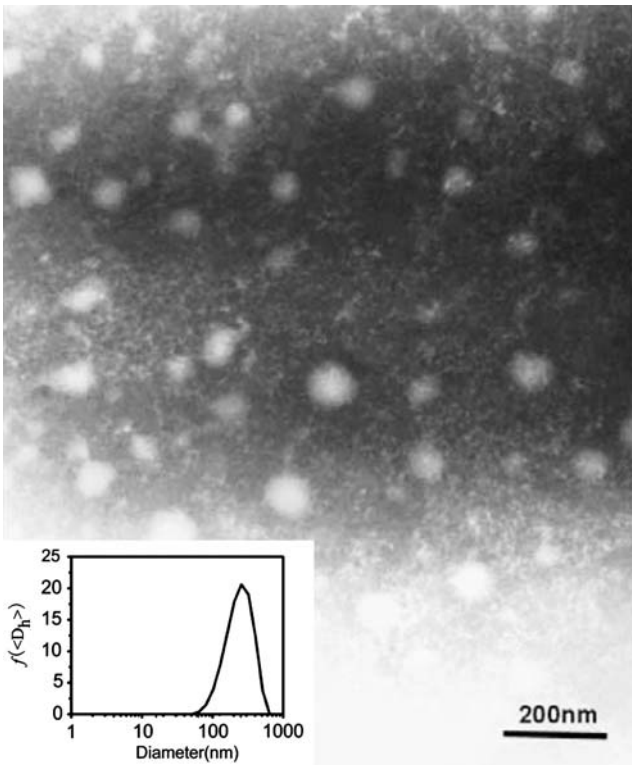

Fig. 1 The negative stained TEM images of DANP. The inset is the distribution of dynamic diameter (D_h) of DANP

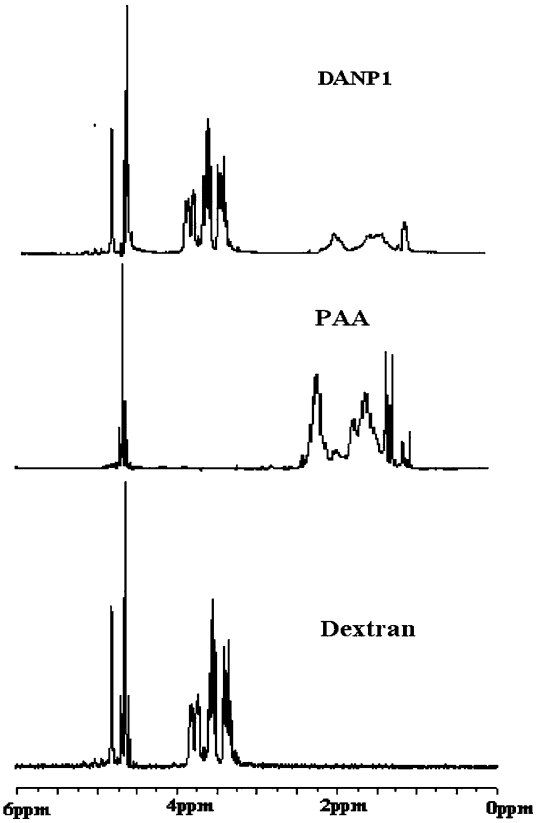

Fig. 2 The ^{1}H NMR spectrum of Dextran, PAA, DANP1 at pH = 12

as well as the inclusion of carboxyl groups in the interior of DANP1.

The mechanism of this synthesis of dextran-based nanoparticles could be proposed as follow: After initiation of graft copolymerization of AA from dextran, the "micelle"-like nano-aggregates form attributed to the complexation between dextran and PAA. As no macroscopic precipitation take place in this process, we suggest that the dextran chains with less complexed segments may still keep solvated and thus stabilize the complex aggregates. Subsequently, participation of crosslinker-MBA leads to further fixation of the structure. Thanks to the shielding effect of superfluous polysaccharide or PAA segments in periphery, the inter-particle crosslink was prevented. Thus the stable nanoparticles instead of the macro-gel formed.

The synthesis of dextran-based magnetic nanocomposites is illustrated as Scheme 1.The TEM images and

hydrodynamic diameters distributions of DAMNP prepared from DANP1 are shown in Fig. 3. After comparing the TEM and DLS results of DAMNP with that of DANP (Fig. 1), it is clear that both DANP and DAMNP possess an irregular spherical morphology with a dimension of 100–200 nm. The diameter of nanocomposites observed by TEM is slightly smaller than that determined by DLS, which should be caused by the shrinkage of nanocomposites after water evaporation as mentioned above [24]. Due to their low density, the DANP are almost invisible under TEM without negative staining, therefore the TEM image of DAMNP displayed in Fig. 3 demonstrates that by this in-situ synthesis, the magnetite nanoparticles with a diameter of ca. 10 nm were encapsulated inside the DANP template, which made the DAMNP nanocomposite visible under TEM. Moreover, the DAMNP particles don't look like spherical particles as shown in Fig. 1 for DANP particles, which should due to inhomogeneous distribution of carboxyl groups in DANP host and the resultant magnetite in DAMNP.

The crystallite phase of the iron oxide can be further characterized by XRD. In order to depress the possible interference of organic composition on the XRD spectrum of iron oxide, the solid DAMNP was burnt from room temperature to 800 °C under a nitrogen atmosphere to degrade the organic composition. The XRD spectra of DAMNP before and after burnt were shown in the inset of Fig. 4. It is clear that the diffraction peaks of magnetite nanoparticles in DAMNP were mostly depressed because of the higher organic content in the samples, which is similar to the XRD result of dextran-magnetite composites [23]. Whereas in the XRD spectrum of DAMNP after burnt, the position and relative intensity of main peaks match well with those from the JCPDS card (19-0629) for magnetite, and the six characteristic peaks occur at 2θ of 30.1, 35.4, 43.0, 56.9 and 62.4 were distinct, indicating that magnetite rather than other kinds of iron oxide was produced.

TGA analysis provides us the information about the composition of DAMNP. As shown in Fig. 5, the thermogram of DANP exhibits three decomposition stages. The first one (below 100 °C) is due to the loss of bound water, and the second one in the range of 250–350 °C is attributed to the degradation of saccharide structure [9], the third decomposition stage in the range of 350–500 °C is a result of the degradation of the residual polymer segments. Comparing the thermogram of DAMNP with that of DANP, the thermogram decreases more sharply during the first stage, which means there is more bound water in DAMNP. Besides, though DAMNP contains magnetite, we propose it should have similar thermal stability with DANP before 350 °C because the degradation in this stage only has relationship with dextran, the same component in DAMNP and DANP. Moreover, the new decomposition stage around 650 °C may be attributed to the interaction between carboxy groups and magnetites nanoparticles which postpone the decomposition of the carboxyl group in PAA segments. Because the remainder of DAMNP as the temperature higher than 600 °C was composed with most Fe_3O_4 and little carbide, and the weight of the carbide from dextran can be known from the weight loss curves of pure DANP, it can be calculated that the weight percentage of Fe_3O_4 in DAMNP is about 15.3%. But the content of Fe_3O_4 calculated from initial reactant is 18.9%, which is slightly

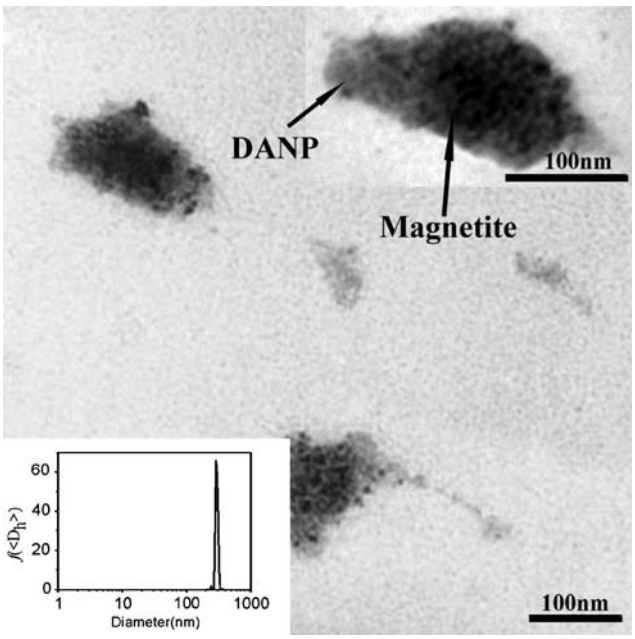

Fig. 3 TEM images of DAMNP. The inset is the amplificatory image of DAMNP and the distribution of dynamic diameter (D_h) of DAMNP

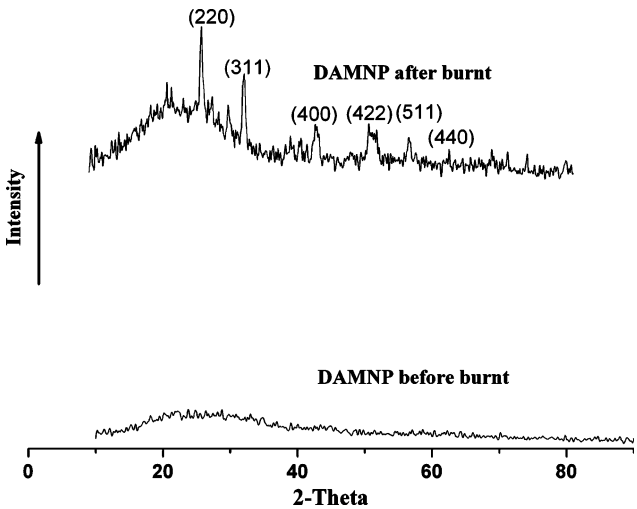

Fig. 4 The XRD patterns of DAMNP before and after burnt

higher than that calculated for TGA analysis. The low value of the content of Fe_3O_4 determined by TGA should be due to the reaction of decomposed components of DANP host with magnetite.

As shown in Fig. 6, Magnetization curves of DAMNP measured at 298 K displays almost immeasurable coercivity and remanence, suggesting that individual magnetite nanoparticles are of a single domain. In case of no hysteresis, the initial susceptibility, $\chi_{i=}(dM/dH)_{H\to 0}$, was determined by the size of nanoparitcles. An upper limit for the magnetic size, D_v, can be estimated using the formula as follows: [26]

$$D_v = \left(\frac{18k_BT}{\pi M_s}\sqrt{\frac{\chi_i}{3\varepsilon M_s H_0}}\right)^{1/3}$$

where k_B is the Boltzmann's constant, M_s is the saturation magnetization, T is the absolute temperature, and ε is the particle volume fraction. $1/H_0$ is the point where the high-field linear extrapolation of M versus 1/H crossed the abscissa, and ε is the particle volume fraction. χ_i (the initial susceptibility) was obtained as 0.0446 emu g^{-1} Oe^{-1} from the VSM data by measuring the slope of magnetization near zero field region, $(dM/dH)_{H\to 0}$ for the magnetization curve at 298 K. $1/H_0$ is the point where the high-field linear extrapolation of M versus $1/H$ crossed the abscissa. It can be obtained as 4×10^{-5} Oe^{-1}. As the saturation magnetization obtained from the magnetization curve is ca. 54.5 emu g^{-1} and the particle volume fraction is ca. 5.5% from the TGA data, the average maximum diameter can be estimated as ca. 5.7 nm. For this value is closed to that of single nanoparticles estimated from TEM image, it maybe conclude that the magnetization curve are corresponding to single nanoparticles rather than hybrid particles. Fig 6

As mentioned above, the negative charge of DANP was provided by the carboxyl groups in PAA. When DANP mixed with iron salt solution, the cationic iron ions would be absorbed inside the DANP. After the addition of the mixture into ammonia solution, magnetite nucleated near the carboxyl groups and so that dextran/magnetite nanocomposites were synthesized.

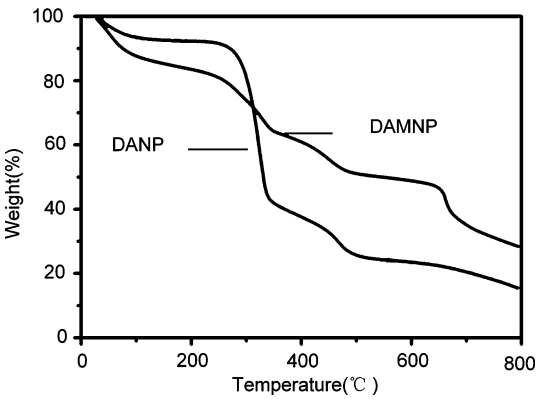

Fig. 5 The thermograms of DANP and DAMNP

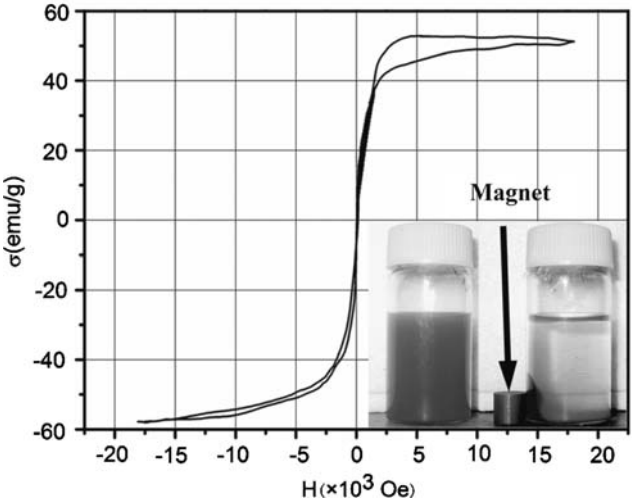

Fig. 6 Magnetization curves of DAMNP. The inset is the photographs of the magnetic behavior of DAMNP aqueous solution

Conclusion

In conclusion, here we presented the one-pot synthesis of dextran-based nanoparticles containing carboxyl groups, as well as the in-situ synthesis of dextran-based magnetic nanocomposites containing Fe_3O_4 nanoparticles. By using dextran-based nanoparticles containing carboxyls as template, the magnetites with a single domain formed homogeneously inside the template via a coprecipitation of ferrous/ferric ions, and the resultant DAMNP have the comparable morphology and diameter with the DANP template. In addition, the DAMNP magnetic nanocomposites exhibit comparable saturation magnetizations to that of reported Fe_3O_4 nanoparticles, which offer them great potential in a large scope of biomedical fields.

Acknowledgements This work was financially supported by *Science and Technology Committee of Shanghai* (Project No. 05ZR14084). We thank Instrumental Analysis Center of SJTU for the assistance on measurements.

References

1. V. BÜTÜN, X. S. WANG, M. V. de PAZ BANEZ, K. L. ROBINSON, N. C. BILLINGHAM, S. P. ARMES and Z. TUZAR, *Macromolecules* **33** (2000) 1
2. S. LIU and S. P. ARMES, *J. Am. Chem. Soc.* **123** (2001) 9910
3. V. M. J. WEAVER, Y. TANG, S. LIU, P. D. IDDON, R. GRIGG, N. C. BILLINGHAM, S. P. ARMES, R. HUNTER and S. P. RANNARD, *Angew. Chem. Int. Ed.* **43** (2004) 1389

4. M. Sauer, W. Meier, Chem. Commun. 2001, 55
5. H. LEE, E. LEE, D. K. KIM, N. K. JANG, Y. Y. JEONG and S. JON, *J. Am Chem. Soc.* **128** (2006) 7383
6. C. L. KAUFMAN, M. WILLIAMS, L. M. RYLE, T. L. SMITH, M. TANNER and CHIEN HO, *Transplantation* **76** (2003) 1043
7. D. CHEN, H. PENG and M. JIANG, *Macromolecules* **36** (2003) 2576
8. H. J. DOU, M. H. TANG and K. SUN, *Macromol. Chem. Phys.* **206** (2005) 2177
9. M. H. TANG, H. J. DOU and K. SUN, *Polymer* **47** (2006) 728
10. H. J. DOU, W. H. YANG and K. SUN, *Chem. Lett.* **35** (2006) 1374
11. U. HÄFELI, W. SCHÜTT, J. TELLER, M. ZBOROWSKI, "Scientific and Clinical Applications of Magnetic Carriers" (Plenum Press, New York, 1997)
12. H. GU, K. XU, C. XU, B. XU, Chem. Comm. 2006, 941
13. S. MORNET, S. VASSEUR F. GRASSET and E. DUGUET, *J. Mater. Chem.* **14** (2004) 2161
14. J. W. CHOI, C. H. AHN, S. BHANSALI and H. T. HENDERSON, Sens. Actuators. B Chem. **68** (2000) 34
15. R. MASSART, *IEEE Trans. Magn.* **MAG-17** (1981) 1247
16. Y. S. KANG, S. RISBUD, J. F. RABOLT and P. STROEVE, *Chem. Mater.* **8** (1996) 2209
17. J. ROCKENBERGER, E. C. SCHER and A. P. ALIVISATOS, *J. Am. Chem. Soc.* **121** (1999) 11595
18. T. HYEON, S. S. LEE, J. PARK, Y. CHUNG and H. B. NA, *J. Am. Chem. Soc.* **123** (2001) 12798
19. S. SUN and H. ZENG, *J. Am. Chem. Soc.* **124** (2002) 8204
20. R. MEHVAR, *J. Control. Release* **69** (2000) 1
21. V. MATSURA, Y. GUARI, J. LARIONOVA, C. GUERIN, A. CANESCHI, C. SANGREGORIO, E. LANCELLE-BELTRAN, A. MEHDI and R. J. P. CORRIU, *J. Mater. Chem.* **14** (2004) 3026
22. Z. H. ZHOU, J. M. XIE, J. MING, H. S. O. CHAN, T. YU and Z. X. SHEN, *J. Appl. Phys.* **91** (2002) 6015
23. K. TAO, H. J. DOU and K. SUN, *Colloid Surface A* **290** (2006) 70
24. Y. W. ZHANG, M. JIANG, J. X. ZHAO, J. ZHOU and D. Y. CHEN, *Macromolecules* **37** (2004) 1537
25. L. WANG, K. TU and Y. LI, *Reactive Funct. Polym.* **53** (2002) 19
26. R. W. CHANTRELL, J. POPPLEWELL and S. W. CHARLES, *IEEE. T. Magn.* **14** (1978) 975